A Shock Tube Study of the Product Branching Ratio for the Reaction $NH_2 + NO$ Using Frequency-Modulation Detection of NH_2

M. Votsmeier, S. Song, R. K. Hanson, and C. T. Bowman*

High-Temperature Gasdynamics Laboratory, Department of Mechanical Engineering, Stanford University, Stanford, California 94305

Received: September 3, 1998; In Final Form: January 13, 1999

The product branching ratio of [$NH_2 + NO \rightarrow N_2H + OH$]:[$NH_2 + NO \rightarrow N_2 + H_2O$] has been determined in the temperature range of 1340−1670 K in a shock tube study with laser photolytic generation of the NH_2 radicals. Sensitive frequency-modulation detection of the NH_2 radical enables experiments with very low initial radical concentrations and, hence, virtually no interference from secondary reactions or dependence on the overall rate coefficient of the reaction. The branching ratio, α, defined as $\alpha = k_{1a}/(k_{1a}+k_{1b})$, increases from 0.42 at 1340 K to 0.53 at 1670 K. Over this temperature range our results can be expressed as $\alpha = 0.5 + (3.36 \times 10^{-4})(T/\mathrm{K} - 1600)$. A detailed error analysis yields an uncertainty in the values of α of ± 0.02 near 1500 K, increasing to ± 0.05 at the temperature extremes.

1. Introduction

In the Thermal De-NOx process invented by Lyon,[1,2] NH_3 is added to high-temperature exhaust gases in order to reduce NO_x emissions. The dominant pathway for NO reduction in this process is the reaction of NO with the NH_2 radical, which proceeds through the two product channels:[3−5]

$$NH_2 + NO \rightarrow N_2H + OH \quad (1a)$$

$$NH_2 + NO \rightarrow N_2 + H_2O \quad (1b)$$

The NH_2 radicals are formed through a radical chain mechanism, mainly by the following reactions:

$$H + NH_3 \rightarrow H_2 + NH_2 \quad (2)$$

$$OH + NH_3 \rightarrow H_2O + NH_2 \quad (3)$$

Reaction 1a serves not only as a major NO-removal reaction but also as a branching step that produces two chain carriers. The N_2H formed in reaction 1a either dissociates directly

$$N_2H \rightarrow N_2 + H \quad (4)$$

or in the presence of oxygen forms an OH radical through the following sequence:

$$N_2H + O_2 \rightarrow HO_2 + N_2 \quad (5)$$

$$HO_2 + NO \rightarrow OH + NO_2 \quad (6)$$

In the presence of oxygen, three additional chain carriers are produced from each H atom formed in reaction 4 by the following sequence:

$$H + O_2 \rightarrow OH + O \quad (7)$$

$$O + NH_3 \rightarrow OH + NH_2 \quad (8)$$

Reaction 1a, followed by reactions 4, 7, and 8, is the major chain-branching step in the mechanism. As this sequence produces four chain carriers, while reaction 1b consumes one radical, it is apparent that the branching ratio, α, defined as $\alpha = k_{1a}/(k_{1a} + k_{1b})$ must be at least 0.25 in order to ensure a self-sustained chain reaction. Owing to the critical role of α in determining the chain-branching character of the overall process, detailed modeling of the thermal De-NOx process shows considerable sensitivity to this parameter.

Due to its importance for De-NOx modeling, a relatively large body of experimental data on the $NH_2 + NO$ reaction has been reported in the literature. The overall rate coefficient seems to be well established, at least for temperatures below 1400 K.[5] There also is good agreement on the branching ratio α at temperatures up to about 700 K. At higher temperatures, in the range most relevant for the De-NOx process (1000−1400 K), there still is considerable uncertainty in the branching ratio. A number of low-temperature direct flash photolysis studies yield a relatively small increase of α with temperature and, when extrapolated to De-NOx temperatures, give values of α well below 0.25.[6−9] As discussed above, such low α values are inconsistent with the De-NOx process being a self-sustaining radical chain process. On the other hand, an early combustion-driven flow reactor study[10] yielded a sharp increase of the branching ratio, α, at temperatures above 1000 K, leading to a value of $\alpha = 0.6$ at 1300 K. Lin and co-workers[11,12] confirmed the sharp increase of α at temperatures above 1000 K. However, a recent reinterpretation of the experimental data in refs 11 and 12 by Park and Lin[13] has resulted in a reduction in the α values at elevated temperatures. Glarborg et al.[14] recently determined the branching ratio, α, in the temperature range of 1211−1370 K from De-NOx flow reactor experiments and found that α increases from about 0.35 at 1211 K to about 0.45 at 1370 K. This result is in agreement with earlier flame speed modeling studies by Vandooren et al.[15] and Brown and Smith.[16]

The objective of this study is to use our newly developed shock tube/frequency-modulation detection scheme in conjunction with laser flash photolytic generation of NH_2 to measure directly the branching ratio, α, at high temperatures in order to resolve the existing disparate results.

10.1021/jp983613v CCC: $18.00
Published on Web 03/02/1999

2. Outline of the Experiments

The high sensitivity of the De-NOx process to the branching ratio, α, makes it difficult to quantitatively predict De-NOx efficiencies and to validate the De-NOx reaction mechanism without using the branching ratio as a fitting parameter in the modeling process. Our approach is to find experimental conditions where we can directly observe the temporal evolution of a process with a chain-branching behavior similar to the full De-NOx process, but with a sufficiently simplified chemistry to allow a determination of α with little sensitivity to secondary reactions. To achieve this we use the following three experimental techniques: (1) a traditional shock-tube technique to produce controlled and uniform high-temperature conditions; (2) laser photolysis to initiate the chain process by instantaneously producing controlled concentrations of chain-branching radicals; (3) frequency-modulation (FM) detection of the NH_2 radical to allow sensitive measurement of the chain carrier radical concentration.

In the experiments, an initial NH_2 radical population is generated by laser flash photolysis of a mixture containing NH_3 and NO diluted in argon:

$$NH_3 + h\nu \rightarrow NH_2 + H \quad (9)$$

The NH_3 concentration is chosen to be sufficiently high so that the H atoms formed during NH_3 photolysis quickly react with excess NH_3 to form NH_2:

$$H + NH_3 \rightarrow H_2 + NH_2 \quad (2)$$

After a few microseconds, an NH_2 concentration of approximately twice the initial NH_2 concentration is established.

Under the present experimental conditions, NH_2 reacts mainly with NO via the two reaction channels 1a and 1b:

$$NH_2 + NO \rightarrow N_2H + OH \quad (1a)$$

$$NH_2 + NO \rightarrow N_2 + H_2O \quad (1b)$$

Since, in contrast to the normal De-NOx process, the mixture does not contain O_2, the N_2H formed in reaction 1a quantitatively decomposes into N_2 and H:

$$N_2H \rightarrow N_2 + H \quad (4)$$

At the high NH_3 concentrations in our experiments, the two reactive radicals resulting from reaction 1a, H and OH, react quickly with excess NH_3 to reform NH_2:

$$H + NH_3 \rightarrow H_2 + NH_2 \quad (2)$$

$$OH + NH_3 \rightarrow H_2O + NH_2 \quad (3)$$

Consequently, each NH_2 radical reacting via the channel 1a leads to the formation of two new NH_2 radicals, while channel 1b is chain terminating and leads to the loss of one NH_2 radical. In this way a chain process is initiated with a branching behavior that is almost entirely controlled by reactions 1a and 1b.

In a simplified treatment, assuming that the rates of reaction 3 and the sequence 4 plus 2 are instantaneous compared to reactions 1a and 1b (due to the high NH_3 concentration), we expect an exponential increase/decrease of the NH_2 concentration with an effective rate coefficient k_{obsd}

$$k_{obsd} = k_{overall}(2\alpha - 1) \quad (10)$$

where $k_{overall} = k_{1a} + k_{1b}$.

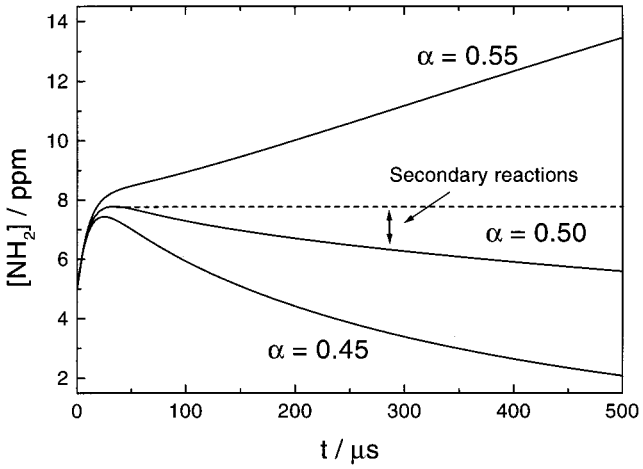

Figure 1. Solid lines: CHEMKIN simulations of NH_2 mole fraction time profiles for three different values of the branching ratio, α, and typical experimental conditions of this study: $[NH_3] = 1\%$, $[NO] = 0.2\%$, $[H]_0 = [NH_2]_0 = 5$ ppm, $T = 1500$ K, $p = 1.3$ atm. Dashed line: eq 10 for the same conditions.

In the special case where $\alpha = 0.5$, k_{obsd} is independent of $k_{overall}$, and the NH_2 concentration will remain at a constant level. Hence, it should be possible to determine α for a small temperature range, where α is close to 0.5, nearly independent of assumptions for $k_{overall}$. For temperatures where α differs from $\alpha = 0.5$, the determination of α will of course begin to show some sensitivity to $k_{overall}$.

The simple kinetic scheme consisting of reactions 1−4 and resulting in eq 10 is useful as it provides intuitive insight into the sensitivity of the measurements to the branching ratio, α, and the overall rate coefficient $k_{overall}$. However, the actual data analysis was carried out using CHEMKIN simulations with the full 129-reaction De-NOx mechanism of Miller and Glarborg[5] with α as a single adjustable parameter to fit the simulations to the experimental NH_2 concentration time profiles. Sensitivity and reaction path analyses for the conditions of the present study show that only a small subset of the complete mechanism contributes to formation and removal of NH_2. Figure 1 shows simulations using the full mechanism for three values of α near 0.5. The simulations clearly demonstrate the high sensitivity of the measurements to the branching ratio. Also shown in Figure 1 is the constant NH_2 concentration profile predicted by the simple kinetic scheme and eq 10 for $\alpha = 0.5$. For the conditions of Figure 1, secondary reactions are responsible for only a small change after the peak in the NH_2 time history. The most important secondary reactions are relatively well-known so that if the measurements are modeled by the full mechanism, the relative error in α caused by uncertainty in the secondary rate parameters for the conditions of Figure 1 can be estimated to be less than 1%.

Figure 2 shows a sensitivity plot for the conditions of Figure 1 with the normalized sensitivity to the branching ratio, α, defined as $S_\alpha = (d[NH_2]/d\alpha)(\alpha/[NH_2]_{max})$, the normalized sensitivity to the overall rate coefficient for reaction 1, $k_{overall}$, and the normalized sensitivities for the most important secondary reactions. The sensitivity plot confirms that the experiments are highly sensitive to the branching ratio and are virtually free of interference from secondary reactions and the overall rate

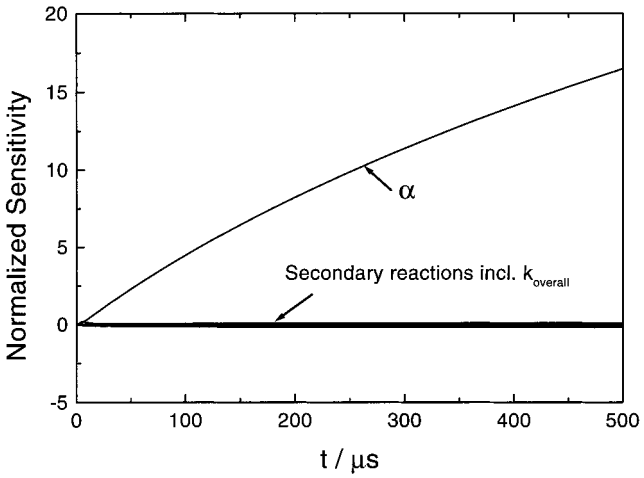

Figure 2. Normalized relative sensitivities $S_\alpha = (d[NH_2]/d\alpha)(\alpha/[NH_2]_{max})$, $S_k = (d[NH_2]/dk)(k/[NH_2]_{max})$, respectively, to the branching ratio α, the overall rate constant $k_{overall}$, and the most important secondary reactions for the experimental conditions of Figure 1.

coefficient. It must be emphasized that these insensitivities result from the low radical concentrations for our experimental conditions, which are made possible by the high sensitivity of the FM detection scheme.

3. Experimental Setup

The experimental setup consists of a conventional shock tube, a photolysis laser, and the FM system for sensitive quantitative detection of NH_2.

3.1. Shock Tube and Photolysis System. The shock tube facility and the laser photolysis setup have been described previously,[17] and only a brief description is presented here.

Experiments were carried out behind reflected shock waves in a stainless steel shock tube with a 6-m long driven section and an internal diameter of 15 cm. Incident-shock velocities were determined using a series of five PCB model 11A36 piezoelectric pressure gauges. Reflected-shock pressure and temperatures were calculated from these velocities using frozen chemistry one-dimensional shock wave theory. An earlier study at similar conditions has shown that, over the reflected shock test time of approximately 1 ms, temperature and pressure vary no more than the experimental uncertainty of 1.5%.[18]

To reduce the uncertainty in the initial NH_3 concentration due to wall adsorption effects, mixtures were prepared continuously by a flow controller system (Hastings 0−3 slpm and Sierra Flow 0−2 slpm) from two commercial gas mixtures containing nominally 1% NH_3 (Praxair) and 2% NO (Praxair), respectively. The NO mixture was analyzed by the manufacturer upon completion of the experiments and was found to contain 86 ppm of NO_2, corresponding to 8.6 ppm of NO_2 in the final mixture. CHEMKIN calculations with the mechanism of Miller and Glarborg revealed that the effect of the NO_2 impurity on the determined branching ratio varies from less than 0.005 at lower temperatures to about 0.02 at higher temperatures. The influence of the small NO_2 impurity was taken into account in the data analysis and for the estimation of the measurement uncertainties. The uncertainty in the reactant mixture composition due to uncertainties in the base mixtures and the mixing process is less than 1%. Before each shock, the shock tube was flushed for at least 10 min with the mixture at the initial pressure of the experiment and the shock was performed with a delay of less than 30 s after the flow was stopped.

For the laser flash photolysis, a Lambda-Physik (Compex 102) ArF excimer laser producing ∼60-mJ pulses at 193 nm was used. The exiting laser beam had a height of ∼2 cm and was expanded in the horizontal plane by a 50-mm focal width cylindrical lens to a width of more than 60 cm. The central part of the expanded beam entered the shock tube, parallel to the shock tube axis through a 14-cm wide and 2-cm high Suprasil window in the end wall. Due to the expansion of the excimer beam and the use of only the central part of the beam for the photolysis experiment the effect of excimer laser beam nonuniformity is greatly reduced. For this setup the beam nonuniformity across the shock tube diameter was less than 3%. The excimer photolysis beam and the frequency-modulated laser beam are carefully aligned to ensure full overlap in the shock tube. The excimer laser was triggered by the last pressure gauge of the shock velocity measurement system and was appropriately delayed so that the heated mixture is photolyzed approximately 30 μs after passage of the reflected shock wave.

3.2. Frequency-Modulation Detection. The development of more sensitive diagnostic techniques for shock tubes enables experiments at lower initial concentrations and, hence, reduced sensitivity to secondary reactions. The introduction of narrow line width laser absorption measurements has allowed considerable progress in this direction.[19] However, even if state-of-the-art laser noise cancellation techniques are applied, classical laser absorption measurements are still subject to the noise caused by the passage of the laser beam through the shock tube itself, such as scattering and beam steering. Frequency-modulation detection, as a differential absorption scheme, is insensitive to these effects and thus potentially allows a considerable improvement in detection sensitivity.

The frequency-modulation (FM) technique in the form applied in this work was first introduced by Bjorklund[20] for the detection of stable molecules. The detection of transient species via FM spectroscopy, in combination with photochemical modulation, has been utilized by Whittaker et al.[21] to obtain spectra of HCO and ND_4. Recently North et al.[22] demonstrated the usefulness of FM detection for time-resolved chemical kinetic measurements. A detailed introduction to the principles of FM spectroscopy and the relation between absorption line shapes and the corresponding FM signals has been given by Bjorklund et al.[23]

Passing a narrow line width laser beam with an optical frequency (ω_L) through an electrooptical crystal and modulating the refractive index of the crystal with an RF frequency (ω_{RF}) results in a phase-modulated laser beam with a central frequency (ω_L) and sidebands with the frequencies $\omega_L + \omega_{RF}$ and $\omega_L - \omega_{RF}$. In the absence of any absorber, each of the two sidebands forms a beat signal with the central band and the two beat signals are displaced in phase by 180° and equal in amplitude, so that they completely cancel and, ideally, no RF amplitude modulation is observed. When the phase-modulated beam propagates through an absorbing medium, differential absorption or phase shift between the two sidebands leads to imperfect cancellation of the two beat signals and, hence, to an amplitude modulation of the laser beam. Shock tube related distortions such as scattering and beam steering influence both sidebands equally and accordingly do not set the limit on the minimum detectable fractional absorption of the experiment.

In the limit of small absorption, dispersion and modulation index the signal detected at the modulation frequency is given by[20]

$$I_{FM} = MI_0[(\delta_+ - \delta_-)\cos\theta + (\phi_- - 2\phi_c + \phi_+)\sin\theta] \quad (11)$$

where M is the sideband modulation index, I_0 is the intensity of the carrier beam, δ_+ and δ_- are the amplitude attenuations at the higher and lower sideband frequencies, respectively, ϕ_-,

ϕ_c, ϕ_+ are the optical phase shifts at the sideband and carrier frequencies, respectively, and θ is the absolute phase between the reference and the beat signal at the mixer. Due to careful alignment of the phase θ to 0° the signal becomes proportional to the differential absorption between the two sidebands only. Absolute concentrations of the detected species can be calculated from the measured signal I_{FM} if the response characteristic of the electronic setup has been calibrated and if the absorption spectrum of the detected transition is known.

We have used the $\tilde{A}^2A_1 \rightarrow X^2B_1(090 \rightarrow 000)\Sigma^pQ_{1,N}7$ doublet lines for the detection of the NH_2 radical. This feature has been previously used for the detection of the NH_2 radical by conventional narrow-bandwidth laser absorption. Its absorption line shape has been measured by rapid scanning laser absorption, and we have recently redetermined its average line strength.[17,24] Furthermore, we have recently measured the FM spectrum of this feature in shock tube experiments and have shown that the measured FM line shape is well reproduced by the line shape calculated from the measured absorption line shape and linestrength.[25] The FM spectrum of the $\tilde{A}^2A_1 \rightarrow X^2B_1(090 \rightarrow 000)\Sigma^pQ_{1,N}7$ overlapping doublet shows two extrema at 16739.79 and 16740.00 cm^{-1}. A carrier wavelength of 16739.79 cm^{-1} was used throughout this work. Details of the calibration procedure for quantitative FM measurements in shock tubes are given in ref 25.

In the experimental setup, a Spectra-Physics model 380 ring dye laser operated with rhodamine 6G dye and pumped with the 4 W all-lines output of a Spectra-Physics model 164 Ar^+ laser was used as the narrow line width laser source. The output wavelength was monitored with a Burleigh WA-10 wavemeter. The probe beam was phase modulated at a frequency of 600 MHz by a Quantum Technology model TWAP-10 nonresonant modulator. Residual amplitude modulation (RAM) in the electrooptic modulator was minimized by careful adjustment of the input polarization of the laser beam and the modulator alignment and was found to form a constant background on the differential output on the time scale of the experiments. The relative intensity of the sidebands as well as the single-mode nature of the carrier beam were monitored with a Spectra Physics model 470 8-GHz scanning interferometer in the transmissive mode. The same interferometer in the reflective mode was used to calibrate the response of the electronic setup by simultaneously measuring the FM and absorption signal of the reflective etalon. Radio frequency power into the phase modulator was adjusted to give first-order sidebands with typically 10−15%, each, of the carrier frequency intensity.

The modulated beam was slightly focused through the shock tube 2 cm from the end-wall, and the transmitted beam with an intensity of 2 mW was focused on a New Focus model 1601 detector with a bandwidth of 1 GHz. The ac signal from the photodetector was filtered by a band-pass filter combination, amplified (Minicircuits ZFL-1000LN) with gain of 24 dB, and demodulated by a double balanced mixer (Minicircuits ZFM-2000). The local oscillator was driven at ω_{RF} with a cable of adjustable length in order to match the phase so that only the absorption part of the FM signal was detected. The output signal was amplified by a factor of 10 by a low-noise amplifier with a bandwidth of 1 MHz (Stanford Research Systems model SR560) and was stored in a laboratory computer for subsequent data analysis.

With our current FM setup a detection limit of 0.5 ppm NH_2 at 1500 K with a bandwidth of 1 MHz (S/N = 1) can be routinely achieved. This corresponds to a minimum detectable absorption of less than 0.01% and is more than 1 order of magnitude lower than the minimum detectivities achieved with the classical narrow line width absorption method[19] (0.1% absorption). Furthermore, in the case of the FM measurements the noise shows a nearly statistical frequency characteristic. This means that even lower minimum detectivities than stated above can be achieved if, as in the current study, the signals vary on a sufficiently long time scale to allow a reduction of the measurement bandwidth. In contrast, the shock tube related noise in classical narrow line width laser absorption measurements has a characteristic low-frequency component that interferes with the time scale of the measurement so that reducing the bandwidth does not improve the signal-to-noise ratio (S/N) as much as expected with purely statistical noise. For this reason FM detection becomes even more favorable compared to classical laser absorption detection if the observed concentration changes take place on a long time scale relative to the detection bandwidth.

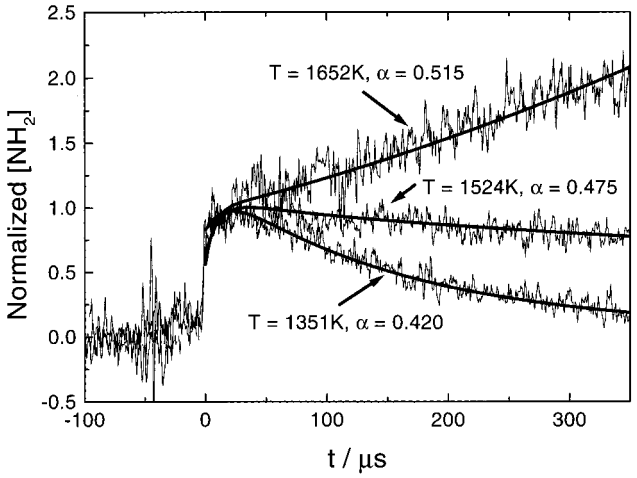

Figure 3. Thin lines: normalized NH_2 concentration time profiles for three different temperatures. Experimental conditions: $[NH_3] = 1\%$, $[NO] = 0.2\%$, $p \cong 1.3$ atm. One arbitrary concentration unit corresponds to NH_2 mole fractions of 5.5, 7.3, and 4.8 ppm at 1351, 1524, and 1652 K, respectively. Bold lines: CHEMKIN fits with α as a single fit parameter.

4. Results and Discussion

Figure 3 shows normalized NH_2 concentration time profiles for three different temperatures. As expected from the simulations described in section 2, a qualitative change in the overall chain-branching behavior from carrier decay at lower temperatures to carrier growth at higher temperatures is observed. The temperature where the NH_2 concentration change switches from negative to positive and where the branching ratio reaches $\alpha = 0.5$ can be determined with very high accuracy to be close to 1600 K. In the temperature range from 1340 to 1670 K, branching ratios were determined by fitting NH_2 profiles using CHEMKIN simulations with α as a single fit parameter. Such simulations are shown along with the corresponding measured concentration traces in Figure 3. Table 1 and Figure 4 present results for the branching ratio as a function of temperature. An increase in α from 0.42 at 1340 K to 0.53 at 1670 K is observed. Over the limited temperature range of the measurements, the branching ratio is well fit by the following linear expression:

$$\alpha = 0.5 + (3.36 \times 10^{-4})(T/\mathrm{K} - 1600) \qquad (12)$$

As pointed out in section 2, in a temperature range where α is approximately 0.5 we expect the determination of the branching ratio to be insensitive both to secondary reactions

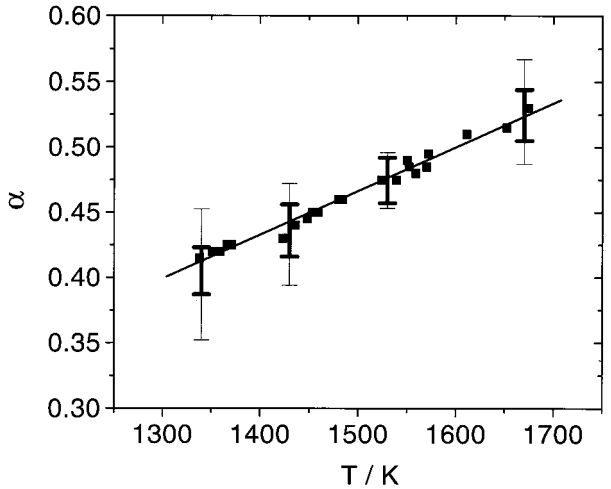

Figure 4. Determined branching ratio, α, as a function of temperature. Thin error bars: estimated uncertainty including measurement errors, uncertainty of secondary reactions, and the effect of the overall rate coefficient $k_{overall}$. Bold error bars: estimated uncertainty not including the effect of uncertainty in $k_{overall}$.

TABLE 1: Measured Branching Ratios as a Function of Temperature

temp (K)	α	temp (K)	α
1338	0.415	1480	0.460
1351	0.420	1484	0.460
1355	0.420	1524	0.475
1356	0.420	1539	0.475
1359	0.420	1550	0.490
1366	0.425	1552	0.485
1371	0.425	1559	0.480
1423	0.430	1570	0.485
1436	0.440	1572	0.495
1448	0.445	1611	0.510
1453	0.450	1652	0.515
1459	0.450	1674	0.530

and to the overall rate coefficient of reaction 1. For temperatures further removed from this point, some sensitivity to the overall rate coefficient $k_{overall}$ is expected. For the data analysis, the overall rate coefficient $k_{ov,M+G}$ from Miller and Glarborg [5] was used:

$$k_{ov,M+G} = (1.3 \times 10^{16})(T/\mathrm{K})^{-1.25} \times \mathrm{mol}^{-1}\,\mathrm{cm}^3\,\mathrm{s}^{-1} \quad (13)$$

The dependence of the determined α values on the assumed overall rate coefficient $k_{overall}$ is shown for different temperatures in Figure 5. If one assumes an uncertainty range for $k_{overall}$ of $0.7k_{ov,M+G} < k_{overall} < 1.5k_{ov,M+G}$, a relative uncertainty in α, induced by the uncertainty of $k_{overall}$, of about 9% at the lower end and of about 7% at the higher end of our temperature range is observed.

Since the uncertainty induced by the overall rate coefficient is relatively large compared to other error sources in the determination of α, we have chosen to fully parametrize the dependence of the determined values α on the assumed overall rate coefficient. Over the temperature range of the measurements and the uncertainty range of $k_{overall}$ specified above, the dependence of the determined α values on the assumed overall rate coefficient $k_{overall}$ is well represented by

$$\alpha = \alpha_{eq12}[1 + (1.169 - (7.168 \times 10^{-4})T/\mathrm{K})y + (-0.931 + (5.723 \times 10^{-4})T/\mathrm{K})y^2] \quad (14)$$

where $y = (k_{overall}/k_{ov,M+G} - 1)$. Equation 14 allows adjustment of the present results, when more precise data on the overall rate coefficient become available. Furthermore, as pointed out in sections 1 and 2, the simplified chain process used to determine α is very similar to the chain process of the actual De-NOx process. Therefore, for consistent De-NOx modeling the present values for α are most advantageously used in combination with the Miller−Glarborg values of $k_{overall}$ that were used to determine the branching ratio from the NH_2 profiles.

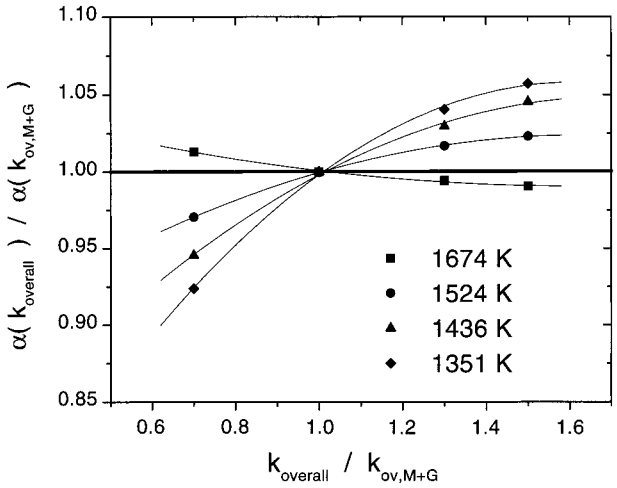

Figure 5. The sensitivity of the determined values for the branching ratio, α, to the overall rate coefficient $k_{overall}$.

Sensitivity calculations indicate that for the temperature range of this study, apart from the overall rate coefficient $k_{overall}$, the only secondary reaction rate coefficient that, when varied within its uncertainty range, significantly affects the determination of α is the rate of the unimolecular decomposition of the NNH radical. This sensitivity is due not so much to a particularly high sensitivity to the lifetime τ_{NNH} of the NNH radical, but rather to the current large uncertainty in τ_{NNH}. While theoretical studies predict a lifetime ranging from 10^{-10} to 10^{-8} s, Miller and Glarborg[5] have pointed out that a lifetime on the order of 10^{-7} s is required in order to consistently model De-NOx behavior. For our data analysis we adopted the value of $\tau_{NNH} = 10^{-7}$ s from Miller and Glarborg, which can be viewed as an upper limit of the possible values for τ_{NNH}. Decreasing the value used for τ_{NNH} in the data analysis to 10^{-8} s leads to slight decrease in the values obtained for α by about 4% at the lower end and by less than 1% at the higher end of our temperature range. For lifetimes below 10^{-8} s, NNH completely dissociates unimolecularly and no further sensitivity to τ_{NNH} is observed. The influence of changing the value of τ_{NNH} used for the data analysis from $\tau_{NNH} = 10^{-7}$ s to a value below 10^{-8} s for the temperature range of our measurements can be represented by

$$\alpha(\tau_{NNH} < 10^{-8}\ \mathrm{s}) = \alpha(\tau_{NNH} = 10^{-7}\ \mathrm{s})[0.993 - 0.0323/(1 + (T/1471.5\ \mathrm{K})^{44.22})] \quad (15)$$

This equation can be used to correct the present results for α if more accurate information on τ_{NNH} becomes available.

In Figure 4 two different sets of error bars are shown. The bold error bars show the estimated uncertainty that includes the statistical error due to measurement uncertainties, the systematic error due to the uncertainty in τ_{NNH}, and the uncertainties involved in taking into account the NO_2 impurity. It does not include any uncertainty resulting from errors in the overall rate coefficient $k_{overall}$. The rationale for displaying these error bars is to show the uncertainty in α when the overall rate coefficient is determined with high enough accuracy so that the error induced in the determination of α becomes insignificant. The

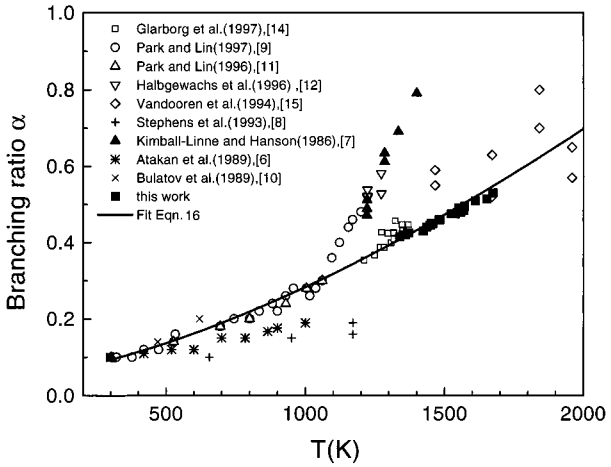

Figure 6. Summary of results for the branching ratio, α, as a function of temperature.

fine error bars in Figure 4 display the error including the uncertainty resulting from $k_{overall}$ if one assumes as an uncertainty range for the overall rate coefficient: $0.7k_{ov,M+G} < k_{overall} < 1.5k_{ov,M+G}$.

Figure 6 shows a summary of the reported data for the branching fraction of the $NH_2 + NO$ reaction. The present values for α are consistent with the results of the recent De-NOx modeling study by Glarborg et al.[14] and the lower temperature data of Park and Lin[9,11] and of Bulatov et al.[7] There is also good agreement with the higher temperature data obtained in a NH_3/NO flame velocity modeling study by Vandooren et al.[15] and Brown and Smith[16] and with the results of a recent shock tube study by Deppe et al.,[26] who determined the branching ratio in the temperature range from 1500 to 2000 K directly from product measurements. A combined fit to these data sets and our data gives the following fit expression for α as function of temperature:

$$\alpha = 0.057 + (7.01 \times 10^{-6})(T/\mathrm{K})^{1.503} \qquad (16)$$

There are obvious discrepancies between this best fit expression and the sharp increase in the branching fraction between 950 and 1200 K reported by Kimball-Linne et al.,[10] Halbgewachs et al.,[12] and Park and Lin.[11] A recent reinterpretation of the higher temperature experimental data of refs 11 and 12 by Park and Lin[13] yield values of α that are in agreement with the present results. Comparison with our results further indicates that the earlier lower temperature studies by Atakan et al.[6] and Stephens et al.[8] seem to have underestimated the increase of α with temperature.

5. Conclusion

A photolytically initiated radical chain process in NH_3/NO/Ar mixtures with an overall branching behavior that is nearly exclusively controlled by the branching ratio of the two reactions

$$NH_2 + NO \rightarrow N_2H + OH \qquad (1a)$$

$$NH_2 + NO \rightarrow N_2 + H_2O \qquad (1b)$$

is described. Shock tube measurements of this chain process allow a precise determination of this branching ratio $\alpha = k_{1a}/(k_{1a} + k_{1b})$. Sensitive frequency-modulation detection of the chain carrier, NH_2, enables experiments with very low initial radical concentrations and, hence, virtually no dependence on secondary reactions and the overall rate coefficient of reaction 1. The branching ratio is found to increase from 0.42 at 1340 K to 0.53 at 1670 K, in good agreement with a recent De-NOx modeling study by Glarborg et al.,[14] with lower temperature measurements by Park and Lin[9,11] and by Bulatov et al.,[7] and with a recent reinterpretation of the higher temperature data in refs 11 and 12.[13]

Acknowledgment. This work was supported by the Department of Energy, Office of Basic Energy Sciences, Division of Chemical Sciences. M.V. thanks the Deutsche Forschungsgemeinschaft for a research fellowship. We are thankful to Trevor Sears and co-workers at Brookhaven National Laboratory for sharing their experience with frequency-modulation kinetics experiments. Discussions with Prof. H. Gg. Wagner and co-workers about the application of FM spectroscopy for shock tube measurements and the helpful assistance of Dr. David Davidson at Stanford are acknowledged.

References and Notes

(1) Lyon, R. K. U.S. Pat. 3,900,554, 1975.
(2) Lyon, R. K. *Int. J. Chem. Kinet*. **1976**, *8*, 315.
(3) Miller, J. A.; Bowman, C. T. *Prog. Energy Combust. Sci.* **1989**, *15*, 287.
(4) Glarborg, P.; Dam-Johansen, K.; Miller, J. A.; Kee, R. J.; Coltrin, M. E. *Int. J. Chem. Kinet*. **1994**, *26*, 421.
(5) Miller, J. A.; Glarborg, P. *Springer Ser. Chem. Phys.* **1996**, *61*, 318.
(6) Atakan, B,; Jacobs, A.; Wahl, M.; Weller, R.; Wolfrum, *J. Chem. Phys. Lett*. **1989**, *155*, 609.
(7) Bulatov, V. P.; Ioffe, A. A.; Lozovsky, V. A.; Sarkisov, O. M. *Chem. Phys. Lett*. **1989**, *161*, 141.
(8) Stephens, J. W.; Morter, C. L.; Farhat, S. K.; Glass, G. P.; Curl, R. F. *J. Phys. Chem.* **1993**, *97*, 8944.
(9) Park, J.; Lin, M. C. *J. Phys. Chem*. **1996**, *100*, 3317.
(10) Kimball-Linne, M. A.; Hanson, R. K. *Combust. Flame* **1986**, *64*, 337.
(11) Park, J.; Lin, M. C. *J. Phys. Chem*. **1997**, *101*, 5.
(12) Halbgewachs, M. J.; Diau, M. J.; Mebel, A. M.; Lin, M. C; Melius, C. F. *26th Symposium (Int.) Combustion*; The Combustion Institute: Pittsburgh, PA, 1996; p 2106.
(13) Park, J.; Lin, M. C. *J. Phys. Chem*. Submitted for publication.
(14) Glarborg, P.; Kristensen, P. G.; Dam-Johansen, K.; Miller, J. A. *J. Phys. Chem. A* **1997**, *101*, 3741.
(15) Vandooren, J.; Bian, J.; van Tiggelen, P. J. *Combust. Flame* **1994**, *98*, 402.
(16) Brown, M. J.; Smith, D. B. *25th Symposium (Int.) Combustion*; The Combustion Institute: Pittsburgh, PA, 1994; p 1011.
(17) Kohse-Höinghaus, K.; Davidson, D. F.; Chang, A. Y.; Hanson, R. K. *J. Quant. Spectrosc. Radiat. Transfer* **1989**, *42*, 1.
(18) Chang, A. Y.; Rea, E., Jr.; Hanson, R. K. *Appl. Optics* **1987**, *26*, 885.
(19) Hanson, R. K. In *Proceedings of the 19th Shock Tube Symposium*; Marseille, 1993; p 7.
(20) Bjorklund, G. C. *Opt. Lett*. **1980**, *5*, 15.
(21) Whittaker, E. A.; Wendt, H. R.; Hunziker, H. E.; Bjorglund, G. C. *Appl. Phys. B* **1984**, *35*, 105.
(22) North, S. W.; Ruian, F.; Sears, T. J.; Hall, G. E. *Int. J. Chem. Kinet*. **1997**, *29*, 127.
(23) Bjorklund, G. C.; Levenson, M. D.; Lenth, W.; Ortiz, C. *Appl. Phys. B* **1983**, *32*, 145
(24) Votsmeier, M.; Song, S.; Davidson, D. F.; Hanson, R. K. Submitted for publication.
(25) Votsmeier, M.; Song, S.; Hanson, R. K submitted for publication.
(26) Deppe, J.; Fiederichs, G.; Ibrahim, A.; Romming, H.-J.; Wagner, H. Gg. *Phys. Chem. Chem. Phys.* **1999**, *1*, 427.